https://ntrs.nasa.gov/search.jsp?R=19780024883 2020-03-22T02:07:34+00:00Z

HELICOPTER NOISE RESEARCH AT THE LANGLEY V/STOL TUNNEL

Danny R. Hoad
Structures Laboratory, U.S. Army R&T Laboratories (AVRADCOM)

George C. Greene
NASA Langley Research Center

SUMMARY

An investigation of the noise generated from a 1/4-scale AH-1G helicopter configuration was conducted in the Langley V/STOL tunnel. Microphones were installed in positions scaled to those for which flight-test data were available. Model and tunnel conditions were carefully set to properly scaled flight conditions. Data presented in this paper indicate a high degree of similarity between model and flight-test results. It was found that the pressure time history waveforms are very much alike in shape and amplitude. Blade slap when it occurred seemed to be generated in about the same location in the rotor disk as on the flight vehicle. If model and tunnel conditions were properly matched, including inflow turbulence characteristics, the intensity of the blade-slap impulse seemed to correlate well with flight.

INTRODUCTION

Helicopter rotor noise is typically separated into categories, such as rotational noise, broadband turbulent interaction noise, and impulsive noise (see ref. 1). When present, impulsive noise is usually the most objectionable for the community and represents a significant problem for reducing ground detectability of military helicopters. It can occur during high-speed flight as a result of the relatively high advancing blade tip Mach numbers or during partial power descent as a result of the interaction of a blade with a vortex generated by a prior blade passage.

One of the most definitive papers on source identification of the blade-vortex interaction (blade slap) type of impulsive noise was published by Tangler (ref. 2). He has demonstrated that blade-vortex interaction can induce local supersonic flow about the blade's lower surface and linked this observed flow condition with measured blade slap.

Rotor noise research at the Langley V/STOL tunnel has focused on the blade-slap impulsive noise source. A completely instrumented model rotor system is available for testing various rotor systems of interest (ref. 3). On-line computing capability and off-line data reduction required for efficient and safe operation of rotor systems are very similar in concept to those used by other facilities involved in rotor sytem research (ref. 4). The unique capability of the V/STOL tunnel to quickly convert to an open throat test chamber and its low background noise level provided an extension of its usefulness as an aero-acoustic facility. Initial tests of the rotor system model in the V/STOL

tunnel were designed to demonstrate the feasibility of conducting rotor noise research in the facility (ref. 5).

The investigation described in this paper was conducted using a model of a helicopter known to generate intense blade slap and for which an extensive flight data base exists (ref. 6). The characteristics of the blade-slap signature are discussed as it affects the spectral content of the overall noise signature measured during the model tests. The primary objective of this paper is to present a comparison of model and flight recorded pressure time histories at properly scaled flight conditions and to discuss the acceptability of using model data to study the noise characteristics of the AH-1G helicopter.

SYMBOLS

The units used for physical quantities defined in this paper are given in both the U.S. Customary Units and the International System of Units. Most quantities were obtained using the U.S. Customary Units. Conversion factors used between these systems are provided in reference 7.

b	number of blades
c	rotor blade chord, m (ft)
C_T	rotor thrust coefficient, $\frac{\text{Thrust}}{\rho\sigma\pi R^2(\Omega R)^2}$
R	rotor disk radius, m (ft)
OASPL	overall sound pressure level, dB (re 2×10^{-5} Pa)
p	acoustic pressure, Pa (lb/ft^2)
SPL	sound pressure level, dB (re 2×10^{-5} Pa)
V_f	tunnel velocity corrected, or true airspeed, knots
V_∞	tunnel velocity, knots
V	rotor tip speed, m/sec (ft/sec)
Ω	rotor rotational speed, rpm
ρ	free-stream density, kg/m^3 ($slugs/ft^3$)
σ	rotor solidity, $bc/\pi R$

APPARATUS AND TEST TECHNIQUE

The model to flight comparison described in this test used the General Rotor Model System (GRMS) at the Langley V/STOL tunnel configured as an AH-1G helicopter without tail rotor. An aerodynamic investigation of this model

without main rotor is described in reference 8. The fuselage had to be enlarged from a 1/4-scale version laterally only to accomodate the GRMS motor and transmission assembly. The model had a 3.35-m (11.00-ft) diameter teetering rotor system scaled from the AH-1G flight vehicle. (See ref. 9.) The blades used a modified NACA 0012 airfoil section and had 10° of washout. A photograph of the model installed in the Langley V/STOL tunnel is presented in figure 1(a), and a photograph of the flight vehicle used in reference 6 is presented in figure 1(b). Microphones were installed on the nose, wings, and tail surfaces of this vehicle for inflight noise measurements. A complete description of the flight test can be obtained from reference 6.

The Langley V/STOL tunnel has a test section that is 4.42 m (14.50 ft) high and 6.63 m (21.75 ft) wide. The semi-anechoic characteristics of the test section are provided by raising the test-section walls and ceiling and are enhanced by treating the floor and ceiling from 5.41 m (17.75 ft) ahead of the model to 2.51 m (8.25 ft) behind the model with 10.16 cm (4.00 in.) thick open-cell polyurethane foam. (See fig. 1(a).) The ceiling surface in the raised position was about 4.7 m (15.4 ft) above the rotor system.

INSTRUMENTATION

The acoustic sensors used for these tests were 1.27-cm (0.50-in.) diameter condensor microphones fitted with standard nose cones. Five microphones were positioned in the flow around the model as presented in figure 2. Three microphones were mounted to the fuselage in locations scaled from positions used on the flight-test vehicle (ref. 6). These microphones can be seen in figure 1(a). The acoustic recording system was consistent with that described in reference 5. All five microphone signals were recorded with a rotor-blade azimuth indicator and time code on a 14-channel frequency-modulated (FM) tape recorder.

The basic frame of the rotor model is completely instrumented for measurement of rotor loads (six-component strain-gage balance) and complete model loads. This plus complete rotor collective and cyclic remote controls (ref. 3) provides complete, precise knowledge of the rotor performance characteristics during the acoustic investigation.

Both flight test and model test provided a blade azimuth position indicator in the form of an electronic blip generated at the vehicle and recorded on the acoustic FM recorder when the instrumented blade passed over the tail cone of the vehicle. This 1/rev blip is indicated in all pressure time histories presented herein.

MODEL-FLIGHT SCALING

To properly match flight-test operating conditions, the tunnel model must be operated with certain parameters matched. Full-scale Reynolds number matching is always desirable, but impossible in this type of model test. Other items suggested in reference 10 as being important to proper performance modeling of rotor systems are blade elasticity and rotor solidity. Unfortunately, these blades were not elastically scaled. The rotor tip speed (V_T),advance ratio, and

thrust coefficient are parameters which must be maintained to provide scaled wake effects on the rotor system or the fuselage. Due to structural limitations in the rotor blades and hub, the full-scale tip speed (227.5 m/sec (746.4 ft/sec)) could not be exactly matched. The required rotor speed Ω (1296 rpm) for this tip speed could not be tested but was set at 1200 rpm. This resulted in a tip speed reduction to 210.7 m/sec (691.2 ft/sec). The advance ratio (V_∞/V_T), however, was carefully matched to the quoted flight-test advance ratio. In this case, the tunnel free-stream velocity was reduced from the flight velocity by:

$$V = V_f \frac{V_{T(model)}}{V_{T(flight)}} = V_f \; 0.925$$

The forward speed values quoted for model data in this paper are corrected by this factor. The flight-test data presented in reference 6 are at various indicated airspeeds at various altitudes. Flight records provided Langley concerning these data provide some information about the pressure altitude. The forward speed values quoted for flight data in this paper are corrected for this pressure altitude. In some cases, gustiness (especially at low altitude) resulted in an uncertainty in flight speed by as much as ± 5 knots.

Rotor lift was carefully maintained at a scaled value based on matching rotor thrust coefficient

$$C_T = \frac{\text{Thrust}}{\rho\sigma\pi R^2(\Omega R)^2}$$

For a quoted nominal 37.36 kN (8400 lb) weight flight-test vehicle, the scaled model weight (lift) was kept at 2.00 kN (450 lb). The flight records indicated that the estimated gross weight at the beginning of each series of runs was consistently 37.54 kN (8440 lb), but the fuel consumption during each series of runs was not recorded in every case. One series recorded indicated fuel usage of 1.27 kN (285 lb), which results in a scaled weight uncertainty of 68 N (15 lb). This uncertainty in flight vehicle gross weight will affect primarily the rotational noise amplitude and is not considered significant.

Typically, the occurance of blade slap has been found to be a function of flight speed and descent velocity. An assessment of the strength of the intensity of the blade slap is usually obtained by an observer in the cabin of the helicopter. This was performed for the investigation reported in reference 6 and is shown in figure 3. It has been found by many researchers that this observation does not always provide a real assessment of the propagation, or occurrence of blade slap, even if compared with measurements just outside the cabin. It does, however, provide a gross indication of the flight conditions required to bracket the envelope of blade-slap intensity.

The procedure used to establish each flight condition simulation was to set a constant tunnel velocity which would provide the correct matched advance

ratio. At this velocity, the tip-path plane angle of attack was varied until desired descent velocity was obtained as computed from the ratio of overall drag to lift

$$\text{Descent velocity} = V_f \sin\left\{\tan^{-1}\left(\frac{\text{Drag}}{\text{Lift}}\right)\right\}$$

At each of these descent velocities, the model collective and cyclics were varied to trim the model in lift, pitching moment, and rolling moment. When all variables described above were set properly then approximately 30 seconds of information from the microphones was recorded on the FM tape recorder. Corresponding model and tunnel information was recorded on the tunnel computer data acquisition system coincidentally. The information presented in this paper is only a small portion of the data collected as described. At each tunnel velocity tested, background noise measurements were made wtih blades off and rotor hub turning at the test speed (1200 rpm).

NOISE DATA REDUCTION AND PRESENTATION

Only data from the nose and right-wing microphones are presented in this paper. One-third octave analyses were performed on model data over a 16-second averaging time and are presented in figure 4. Narrow band analyses were performed for selected portions of the model data presented. It was performed digitally for 20 revolutions of the rotor at a digitizing rate of 20 000 samples per second, resulting in a constant band width of 20 Hz with a resolution of 10 000 Hz. These are presented in figure 5. Detailed comparisons of pressure time-history between model and flight are provided in figures 6, 7, 8, and 9.

DISCUSSION

Acoustic data recorded during the model test at a flight-speed simulation of about 50 knots is presented in figures 5(a) and 5(b). Pressure time histories are presented on the right side of the figure as a function of descent velocity. These correspond to the information analyzed in one-third octave format as presented in the left side of the figure.

The strong impulse signature indicative of blade slap is present in the pressure time histories, and it is evident that the magnitude of the impulse is a direct function of the descent velocity. The position of the impulse on the trace relative to the 1/rev blip is a function of the location of the source mechanism in the rotor disk. Although difficult to locate accurately, it is obvious that the positon of the source did not vary with descent velocity, indicating that the range in descent velocity caused a vertical displacement in the blade-to-vortex spacing only.

Data recorded from the nose microphone at 50.7 knots simulated flight speed (fig. 4(a)) indicates a suprisingly clean signal at nearly zero descent velocity.

One-third octave analysis of these data shows the obvious high amplitude blade-passage frequency fundamental (40 Hz) with associated harmonics. The broadband high frequency noise, which can be associated with turbulence interaction, in this case is of much lower amplitude (about 35 dB less than the fundamental). The background noise in this case is well under the clean rotor signal except in the 200-800 Hz one-third octave band range. The effect of the blade slap impulse can be seen as an increased amplitude above the third harmonic of the blade-passage frequency. This change in the one-third octave spectrum from a descent velocity of 1.067 m/sec (210 ft/min) to 3.302 m/sec (650 ft/min) was primarily associated with the impulse as generated by the blade vortex interaction. Since the rotor thrust was maintained at about 4.413 kN (450 lb) throughout, the amplitudes of blade passage and the first few harmonic frequencies were unaffected by the blade slap. This indicates that, although the impulse noise was repetitive with blade passage, the energy associated with it is well below the low frequency noise (fundamental blade-passage frequency and its first few harmonics) generated by blade loading.

The data recorded from the right wing microphone at these simulated flight conditions (fig. 4(b)) show the same trends. The pressure time histories are not as clean, but the blade passage is evident. Note the change in amplitude scale of the pressure time histories in figures 4(b) and 4(d). The broadband turbulence interaction noise for near level flight is about 25 dB less than the blade passage frequency amplitude. Background noise in this case is well below the rotor noise throughout the spectrum. The impulsive signature energy again reflects itself in the high frequency range beginning at the fourth harmonic of the blade-passage frequency.

The noise characteristics from the nose microphone and right wing microphone at a simulated flight speed of 71.1 knots (figs. 4(c) and 4(d)) were similar to those at 50.7 knots, except some of the data were contaminated by background noise (200-1250 one-third octave band center frequencies). Bulging of the spectral characteristics is evident to some extent above about 200 Hz due to the blade-slap impulse. In this case, the range of descent velocities encompassed the entire region of the intense blade slap, indicating that the vortex was below the rotor disk at low descent velocities, passed through the disk at moderate descent velocities, and was above the disk at high descent velocities.

It is well known that this blade vortex interaction noise when Fourier-analyzed presents itself as harmonics of the blade-passage frequency, just as the Fourier analysis of a pure repetitive impulsive function. Narrow-band analysis was performed on these data, and four samples are presented in figure 5. At 50.7 knots simulated airspeed and 3.302 m/sec (650 ft/min) descent velocity (fig. 6(a)), the harmonics are evident to above 4000 Hz (over 100 harmonics of blade passage). At 71.1 knots, the impulsive harmonics are evident up to at least 8000 Hz (over 200 harmonics of blade passage). Noise generated by blade loading can also be seen in these figures below about 200 Hz, where it is not affected by descent velocity. Above 200 Hz, that noise which can be associated with blade slap is up to 15 dB higher in magnitude than without blade slap. A subjective response to the two signals in figure 6(a), as demonstrated in figure 4, would probably result in the blade slap case being rated as much more objectionable. It is interesting to note the overall sound pressure level of

these two signals are both 129.5 dB. It is obvious that the low frequency rotational noise is dominating these values, and to provide any comparison with human response to this type of noise, weighting factors must be applied. Langley Research Center is involved in this area (ref. 11).

Model-Flight Test Comparison

Comparison between model and flight test data are presented in figures 6, 7, 8, and 9 for the nose and right wing microphones. Recorded pressure time histories from one revolution of the rotor from each test are presented for comparable flight conditions. The frequency content of the model data spectral analysis must be scaled by rotor speed; however, presenting the pressure time history as a function of rotor revolutions, instead of time, effectively scales this factor. Since the rotor tip speed could not be matched to flight and the thrust was scaled by matching thrust coefficient, the thrust was slightly less than disk loading scaling required. The pressure amplitudes of the model data were corrected by this factor for these comparisons.

It is important to note at this point, again, that the flight velocity presented for the flight-test data are corrected values from quoted indicated airspeed based on limited information about pressure altitude. Flight data include effects of tail rotor operation which was not on the model.

Noise signatures from model and flight at a free-stream velocity of about 50 knots are presented in figure 6 for several descent velocities. At a low descent velocity (figs. 6(a) and 6(b)), blade slap, if present, is difficult to identify. Model and flight comparison for the nose microphone indicate the suprisingly clean signal recorded. The waveform is different for the model, probably caused by blade loading variations from Reynolds number or blade elasticity effects. Comparisons for the right wing microphone show very similar waveforms if the tail-rotor blade-passage spikes were removed from the flight data. In fact, an approximate calculation of the difference in pressure amplitude indicates that the properly scaled model blade-passage frequency amplitude was about 1 dB higher than flight. This difference for the nose microphone was about 5 dB. These characteristics are typical of all the comparisons presented herein.

At a high descent velocity (figs. 6(c) and 6(d)), the impulsive signature from blade-vortex interaction is evident in both tests. Even though the waveform recorded on the model nose microphone is different from flight, the impulse is in about the same location in the signature as in flight-test data relative to the 1/rev blip. This indicates that the source mechanism of blade slap occurred in about the same location on the model as flight. The shape and size of the model impulse is remarkably similar to that from flight test. The high descent rate condition probably would be considered to be objectionable in a subjective analysis; however, figure 3 indicates that blade-slap intensity was rated as very light for this flight condition. This is one flight condition where the slap intensity was not detected by cabin observers.

Similar comparisons between model and flight are presented in figures 7, 8, and 9 for a flight velocity of approximately 70 knots. At a low descent velocity (figs. 7(a) and 7(b)), the flight recorded pressure time history shows a definite blade-vortex interaction which is not present in model data. At a moderate descent velocity (figs. 8(a), 8(b), and 8(c)), model data indicated a weak blade-vortex interaction at nearly the same position as at 50 knots. Flight-test data at nearly the same descent velocity shows a very intense blade slap. These data were recorded at a relatively high altitude in "smooth" air. These tests were also conducted at a lower pressure altitude, 396.2 m (1300 ft), in "bumpy" air. Flight records indicated that measurement of indicated airspeed was uncertain ($\pm$5 knots) due to this turbulence. The relative position of the impulse on the pressure time history did not change, but the amplitude did. Reference 6 suggests that this variation was caused by turbulence interaction with the tip vortex. This condition seems to compare more favorably with model tests. The V/STOL tunnel experiences a relatively larger turbulence factor at this speed than at lower speeds. At the high descent velocity (fig. 9), model data (fig. 9(a)) indicate a maximum for blade slap as does flight data at the low, bumpy air pressure altitude (fig. 9(c)). Flight data at the high, smooth air, pressure altitude (fig. 9(b)) indicate a lower blade slap intensity than at the lower descent velocity (fig. 8(b)). These data indicate that turbulence characteristics inflow to the rotor system can cause considerable variance in the degree of blade-slap intensity in flight and in model testing.

CONCLUDING REMARKS

An investigation of the noise generated from a 1/4-scale AH-1G helicopter configuration was conducted in the Langley V/STOL tunnel. Microphones were installed about the model in positions scaled to those locations for which flight-test data were available. Model and tunnel conditions were carefully set to properly scaled flight conditions. Acoustic data recorded during the model tests indicated that:

1. As expected, blade-slap intensity is a direct function of descent velocity, probably caused by only vertical displacement in the blade-vortex interaction.

2. Spectral analysis of a signal with blade slap shows energy concentration above about the third harmonic of the blade-passage frequency.

3. Narrow-band analysis indicated that the blade-slap impulsive signature showed up as harmonics of the blade-passage frequency up to at least 200 harmonics.

Comparisons between model and flight data have been presented in pressure time history form, properly scaled in amplitude and time. The comparison between model and flight-test noise data indicated considerable similarity in waveform, especially that for the right wing microphone. Difference in amplitude was estimated to be about 5 dB for the nose microphone and about 1 dB for the right wing microphone at the blade-passage frequency. At different flight speeds and descent velocities, the comparisons indicated that:

1. Model scale blade-slap occurrence and location on time history relative to 1/rev blip were similar to those recorded in flight at two descent speeds and at 50 knots flight velocity.

2. Intense blade slap recorded on the microphones at 3.302 m/sec (650 ft/min) descent velocity and 50 knots flight speed was not noted during subjective tests in the flight vehicle cabin.

3. With an approximate flight speed of 70 knots, model scale blade slap was not generated as intensely as in flight at high "smooth air" pressure altitudes.

4. At low, "bumpy air" pressure altitudes, flight test and model test blade-slap intensity and its relationship with descent velocity compared very well.

5. A higher turbulence factor in the V/STOL tunnel at 70 knots than at lower speeds and the comparability of model and flight data at the lower turbulent pressure altitude suggest that turbulence inflow into the rotor system can alter the intensity and the occurrence of blade slap.

REFERENCES

1. Langenbucher, V.: Noise Phenomena With Helicopter Rotors and Possibilities of Noise Reduction. European Space Agency Rep. No. ESA-TT-244, Feb. 1976

2. Tangler, James L. L.: Schlieren and Noise Studies of Rotors in Forward Flight Am. Hel. Soc. Paper 77-33-05, May 1977

3. Wilson, John C.: A General Rotor Model System for Wind-Tunnel Investigations. J. Aircraft, vol. 14, no. 7, July 1977, pp. 639-643

4. Hardy, William G. S.; and Pyne, Edward J.: The Use of Computers in Rotary Wing Testing. AGARD CP-210, Numerical Methods and Wind Tunnel Testing, pp. 4-1-4-12

5. Scheiman, James; and Hoad, Danny R.: Investigation of Blade Impulsive Noise on a Scaled Fully Articulated Rotor System. NASA TM X-3528, 1977

6. Sakowski, P. C., Jr.; Charles, B. D.; Cox, C. R.; and Shockey, G. A.: Noise Measurement Test Results for AH-1G Operational Loads Survey. Bell Hel. Co. Rep. 299-099-831, vols. I and II, Feb. 1976

7. Mechtly, E. A.: The International System of Units - Physical Constants and Conversion Factors (Second Revision). NASA SP-7012, 1973

8. Freeman, Carl E.; and Yeager, William T., Jr.: A Wind-Tunnel Investigation of an Unpowered Helicopter Fuselage Model With a V-Type Empennage. NASA TM X-3476, 1977

9. Finnestead, Rodger L.; Laing, Emmett; Connor, William J.; and Buss, Marvin W.: Engineering Flight Test AH-1G Helicopter (Hueycobra). U.S. Army Aviation Systems Test Activity Rep. No. USAASTA 66-06, April 1970

10. Yeager, William T., Jr.; and Mantay, Wayne R.: Correlation of Full-Scale Helicopter Rotor Performance in Air With Model-Scale Freon Data. NASA TN D-8328, 1976

11. Powell, Clemans A.: Annoyance Due to Simulated Blade-Slap Noise. Helicopter Acoustics, NASA CP-2052, Pt. II, 1978. (Paper no. 23 of this compilation.)

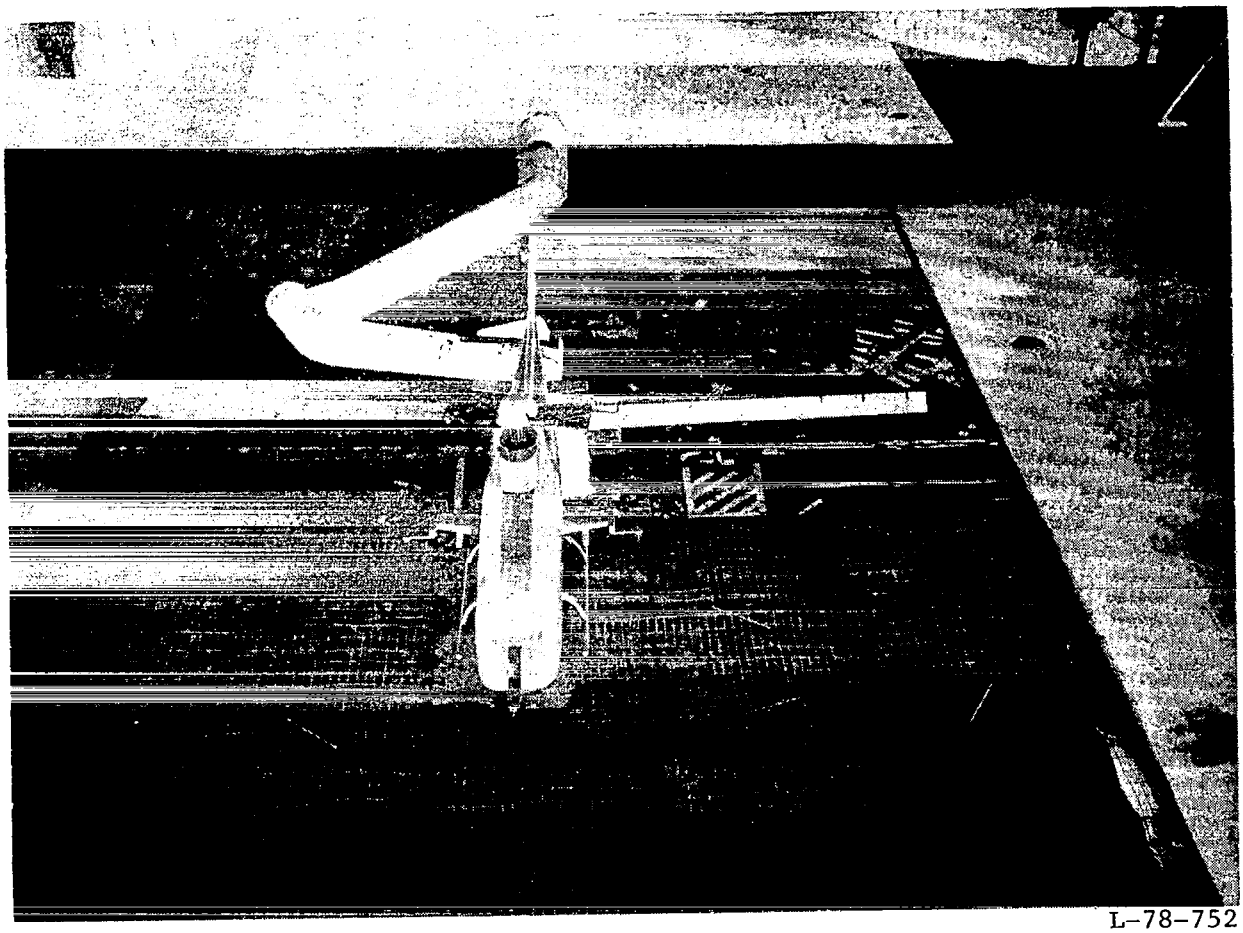

L-78-752

(a) Model installed in Langley V/STOL tunnel.

Figure 1.- AH-1G helicopter.

(b) Flight-test vehicle.

Figure 1.- Concluded.

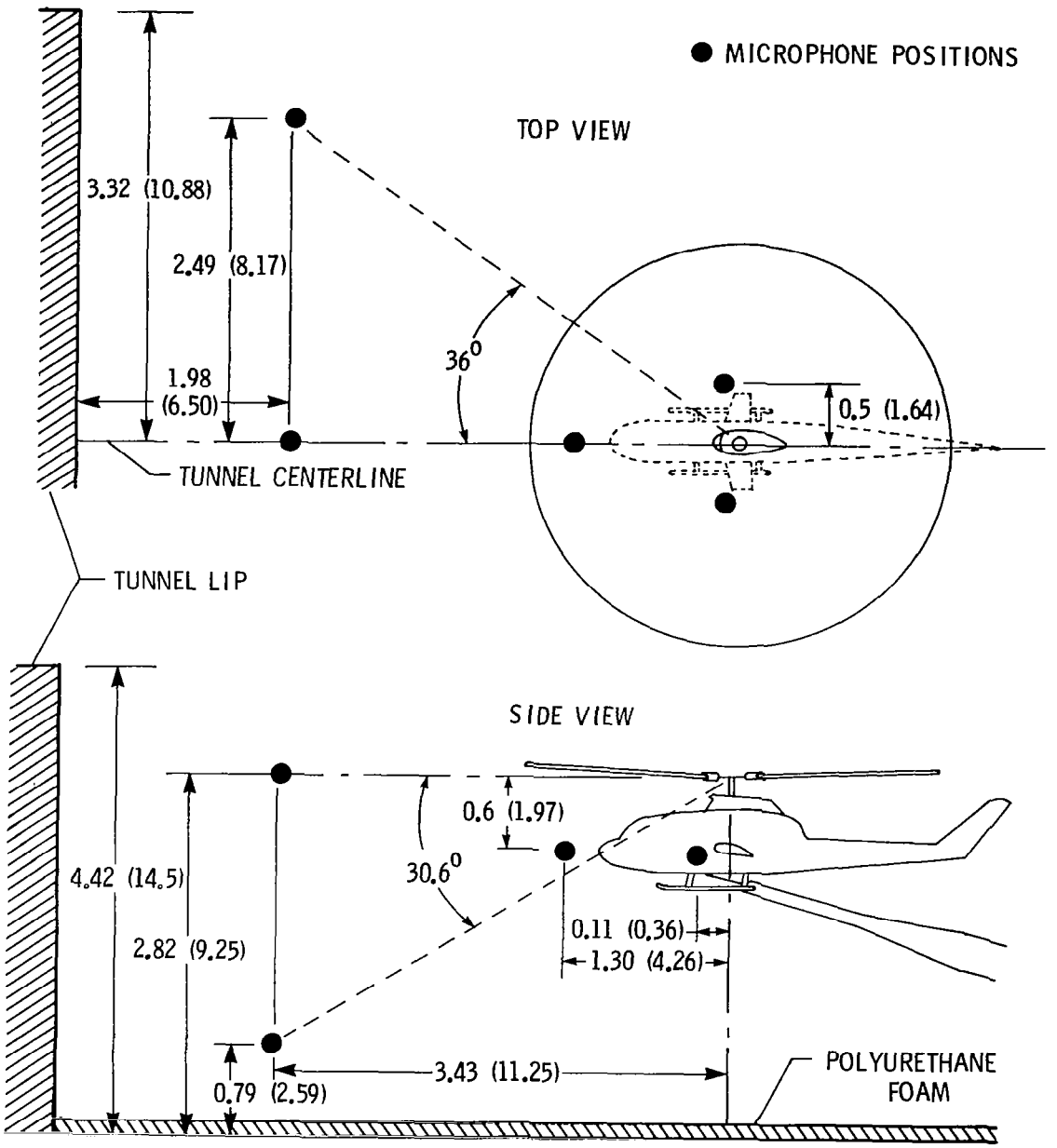

Figure 2.- Model and microphone position in tunnel.
Dimensions in m (ft).

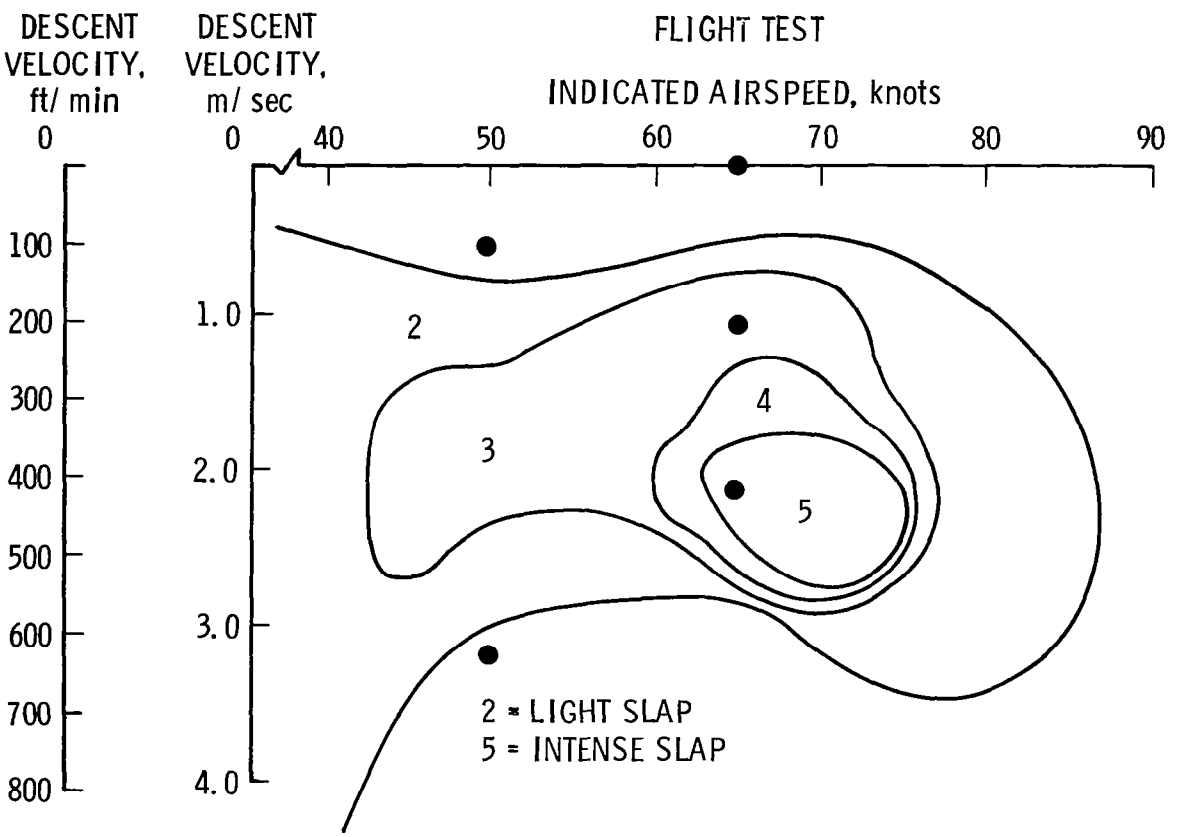

Figure 3.- Internal noise, observer objective response, AH-1G flight test.

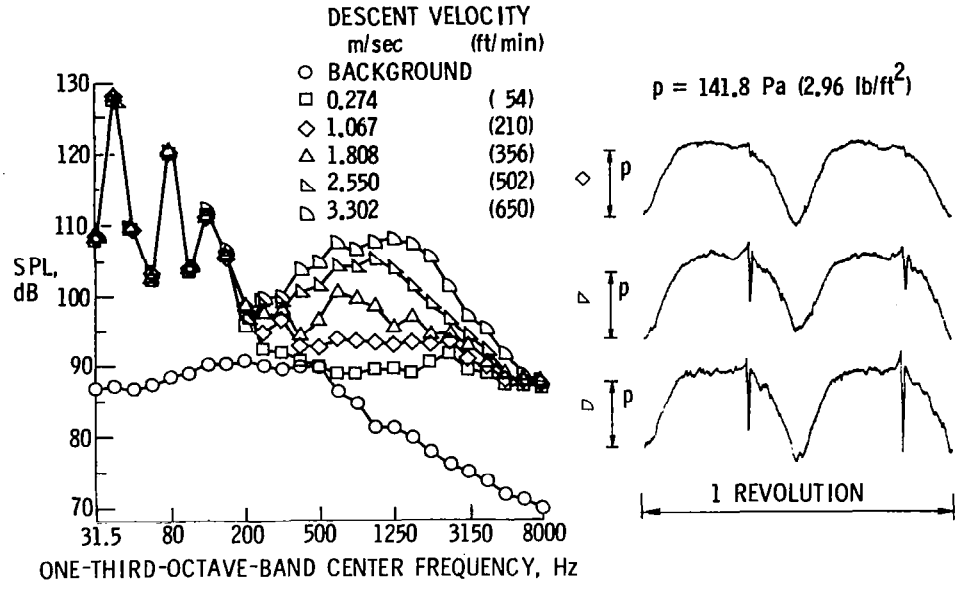

(a) Nose microphone, V_f = 50.7 knots.

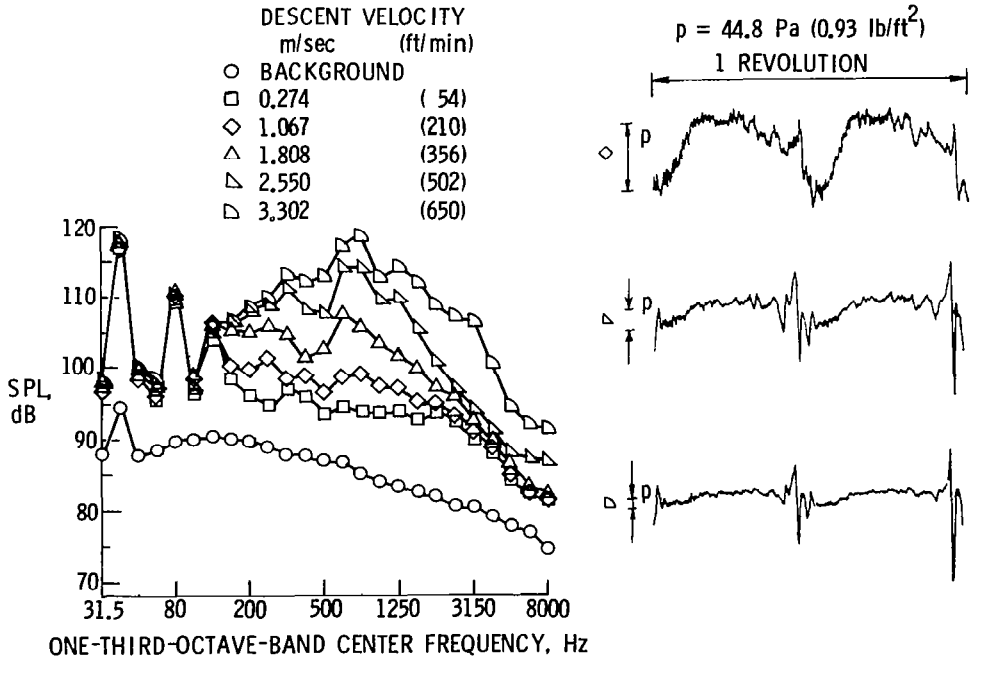

(b) Right-wing microphone, V_f = 50.7 knots.

Figure 4.- Effect of descent velocity on one-third-octave spectrum and time history for model test.

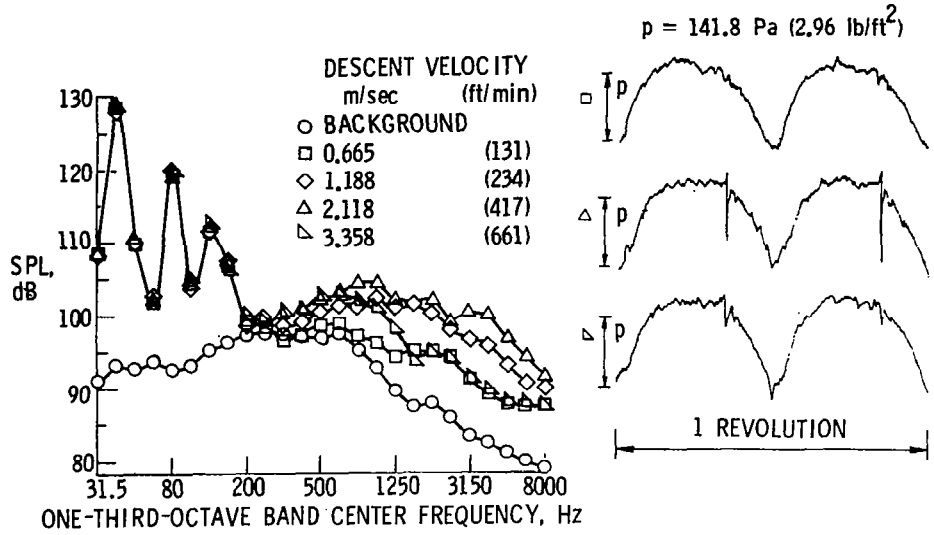

(c) Nose microphone, V_f = 71.1 knots.

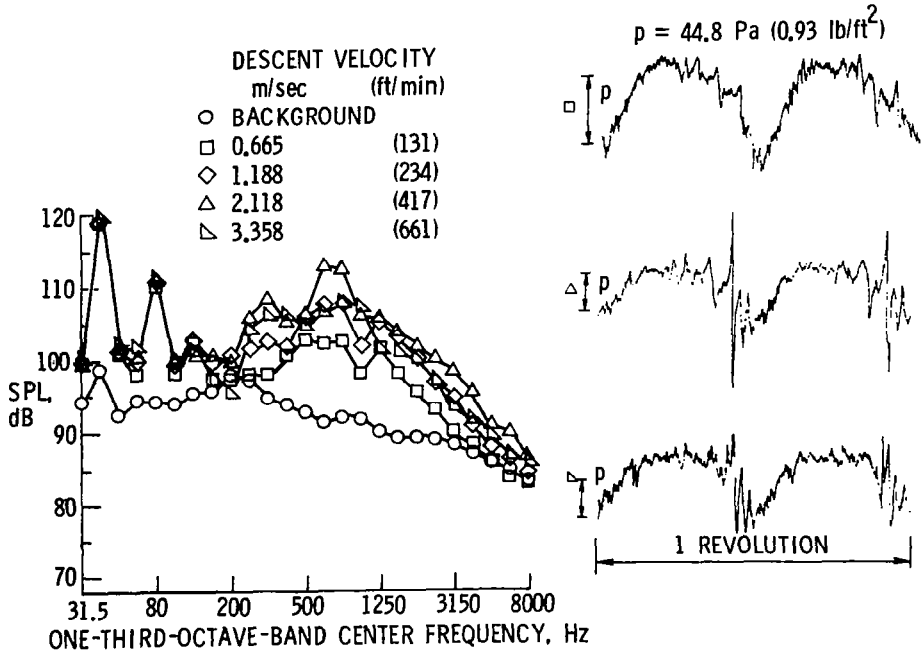

(d) Right-wing microphone, V_f = 71.1 knots.

Figure 4.- Concluded.

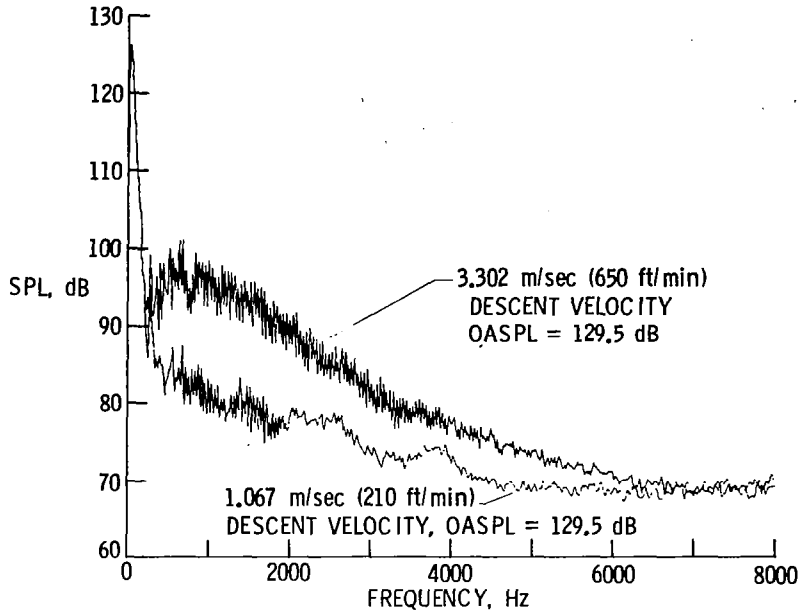

(a) V_f = 50.7 knots.

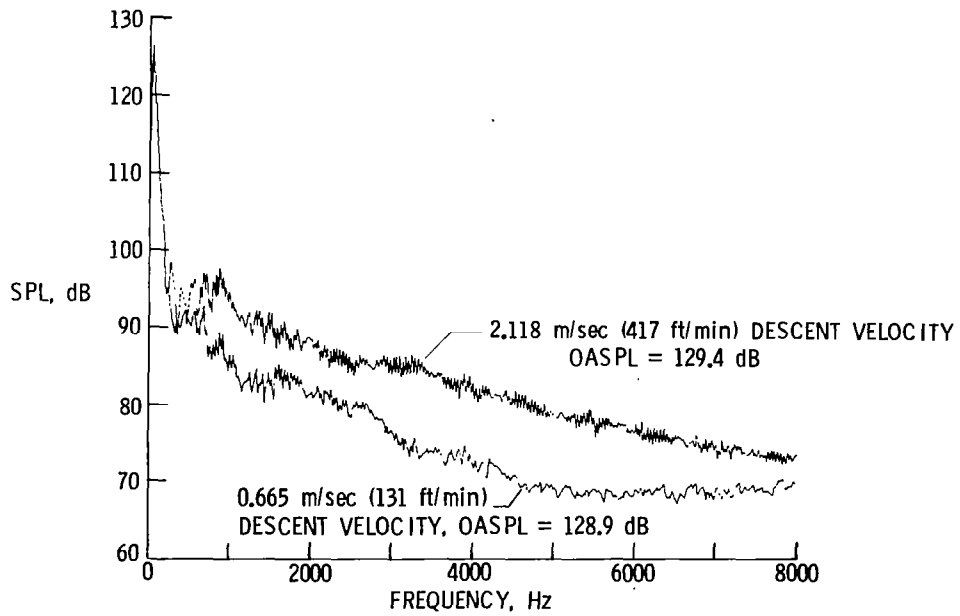

(b) V_f = 71.1 knots.

Figure 5.- Comparison of narrow band analysis of two descent velocities for model tests, nose microphone.

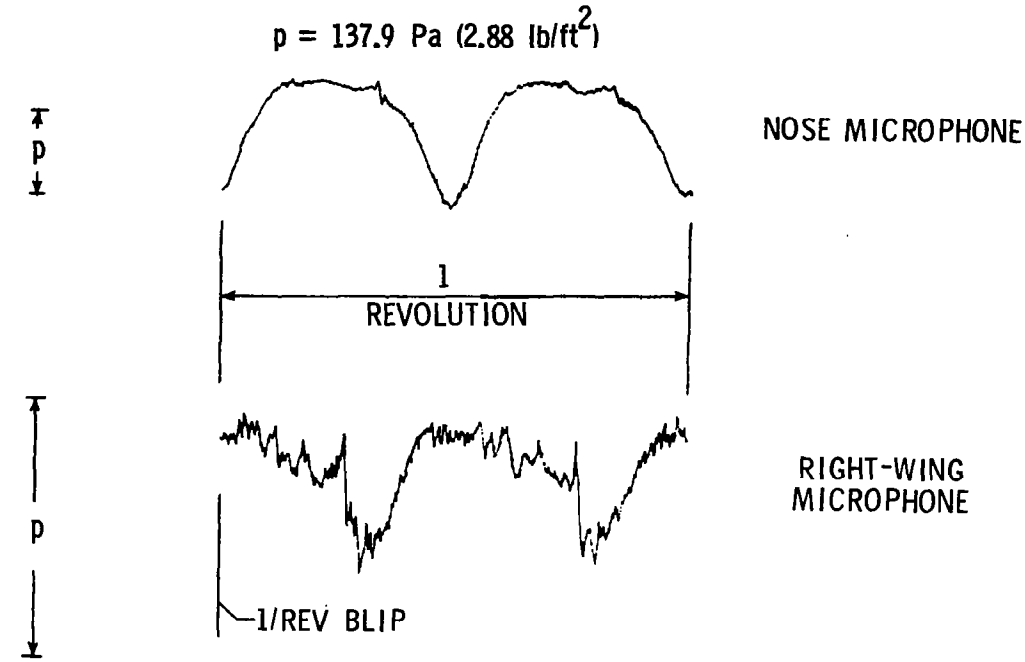

(a) Model data; Descent velocity = 1.067 m/sec (210 ft/min); V_f = 50.7 knots.

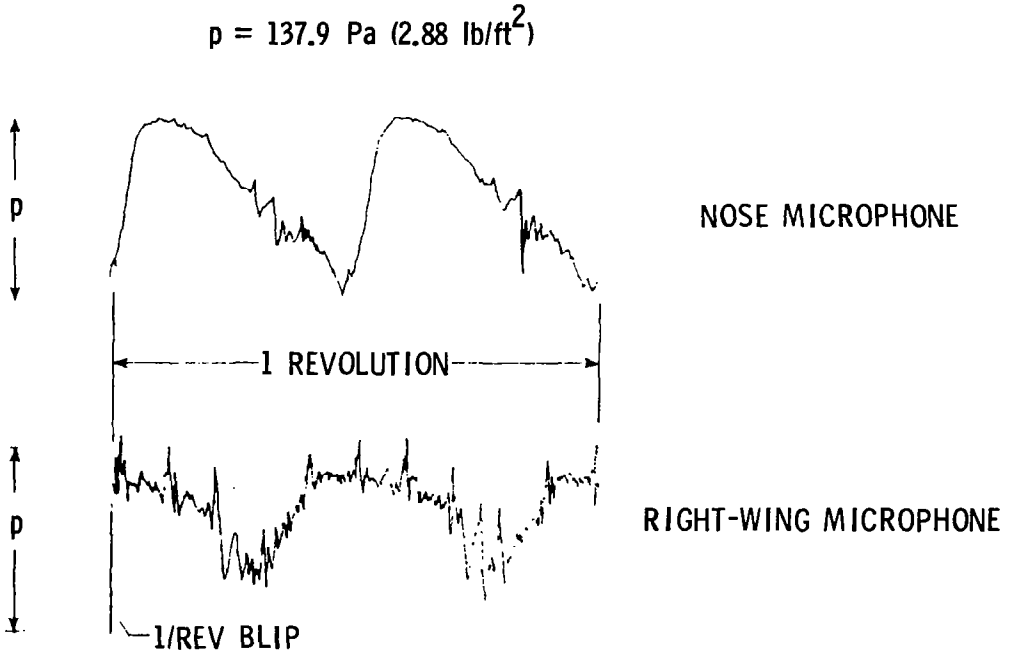

(b) Flight-test data; Descent velocity = 0.508 m/sec (100 ft/min); $V_f \approx 53$ knots.

Figure 6.- Comparison of model and flight recorded acoustic time history for two microphone positions.

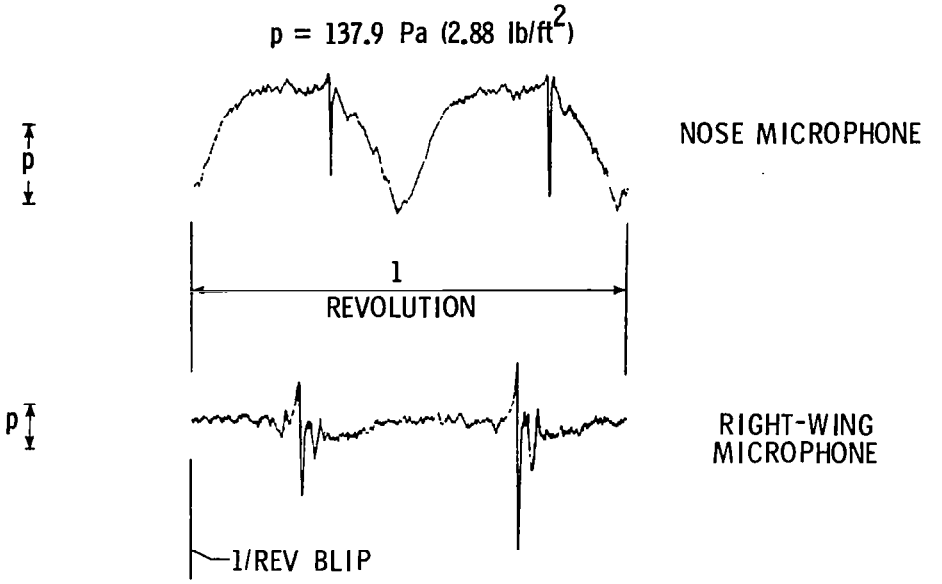

(c) Model data; Descent velocity = 3.302 m/sec (650 ft/min); V_f = 50.7 knots.

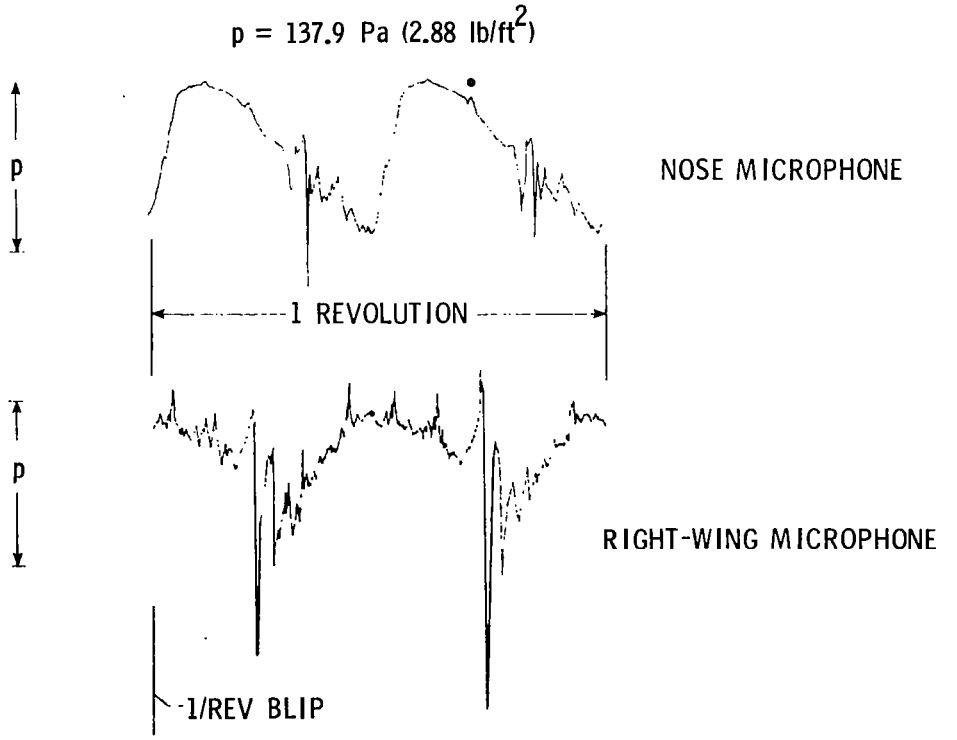

(d) Flight-test data; Descent velocity = 3.048 m/sec (600 ft/min); $V_f \approx 53$ knots.

Figure 6.- Concluded.

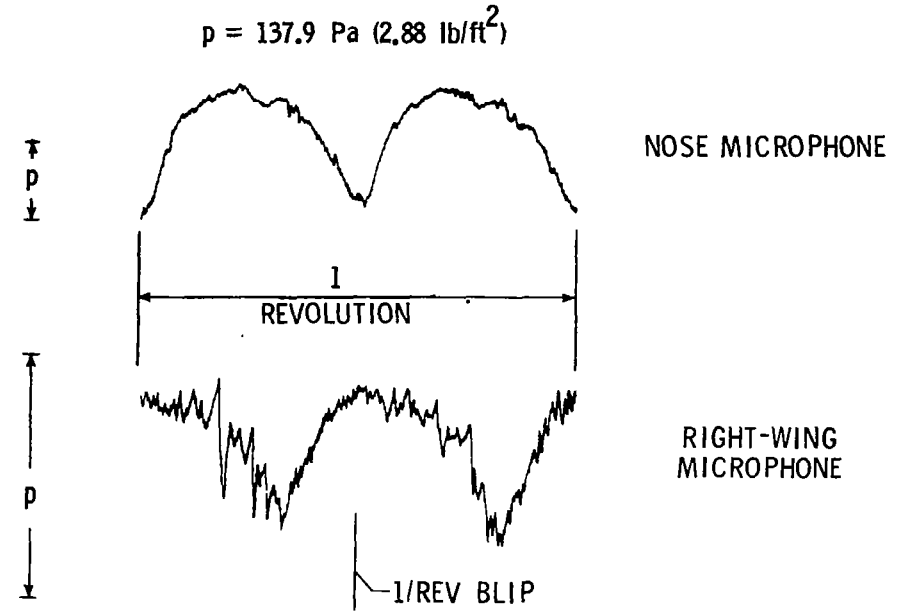

(a) Model data; Descent velocity = 0.665 m/sec (131 ft/min); V_f = 71.1 knots.

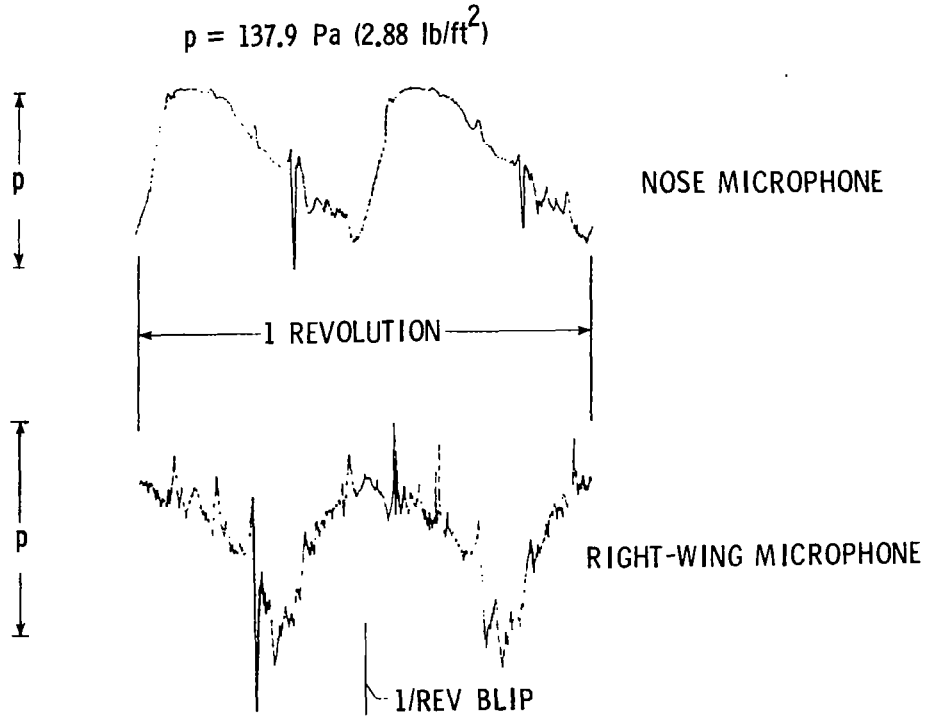

(b) Flight data; Descent velocity = 0 m/sec (0 ft/min); V_f ≈ 68 knots; ≈914.4 m (≈3000 ft) pressure altitude.

Figure 7.- Comparison of model and flight recorded acoustic time history for two microphone positions. Low descent velocities.

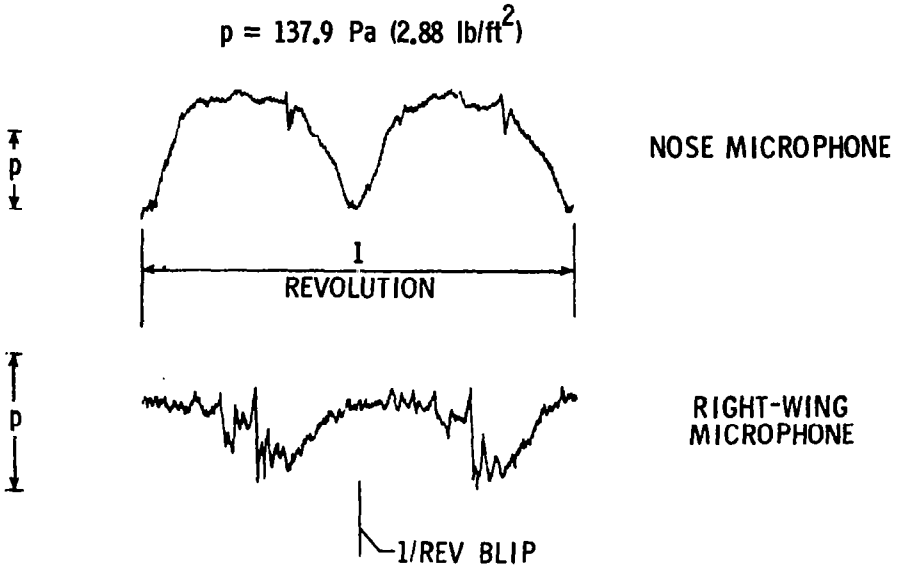

(a) Model data; Descent velocity = 1.188 m/sec (234 ft/min); V_f = 71.1 knots.

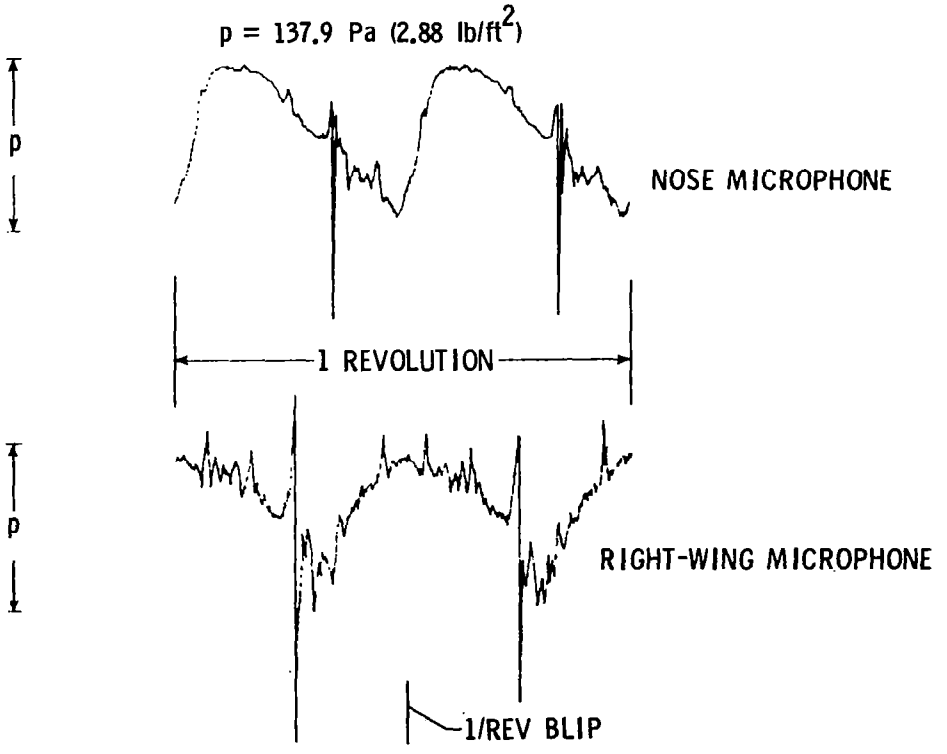

(b) Flight data; Descent velocity = 1.016 m/sec (200 ft/min); V_f ≈ 68 knots; ≈914.4 m (≈3000 ft) pressure altitude.

Figure 8.- Comparison of model and flight recorded acoustic time history for two microphone positions. Moderate descent velocities.

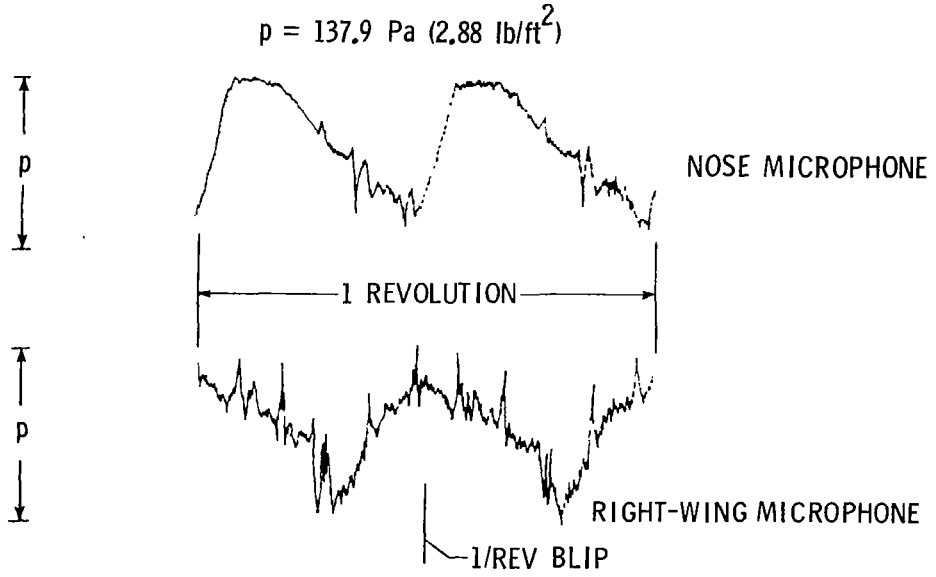

(c) Flight data; Descent velocity = 1.016 m/sec (200 ft/min); $V_f \approx$ 66 knots; ≈396.2 m (≈1300 ft) pressure altitude.

Figure 8.- Concluded.

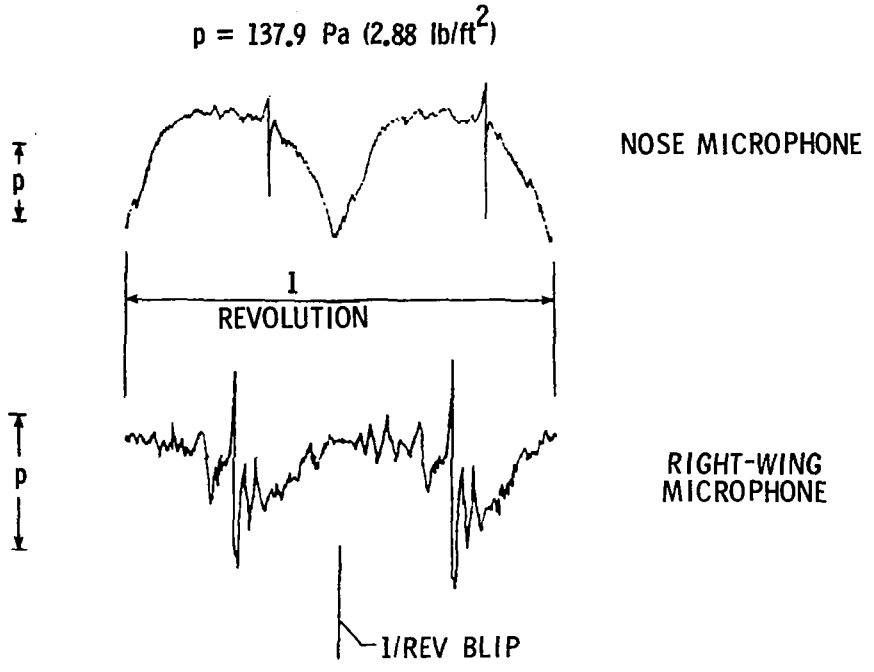

(a) Model data; Descent velocity = 2.118 m/sec (417 ft/min); V_f = 71.1 knots.

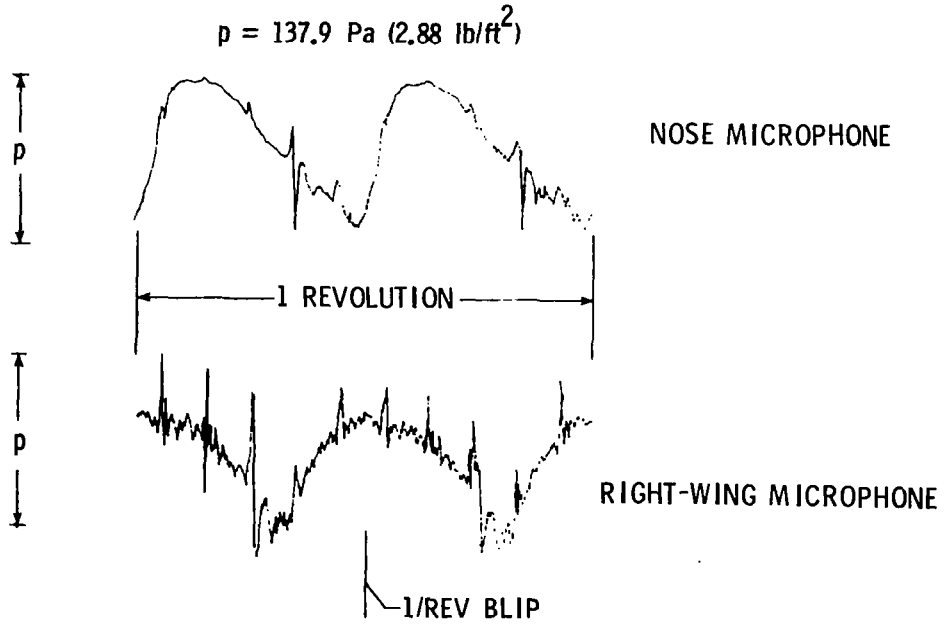

(b) Flight data; Descent velocity = 2.032 m/sec (400 ft/min); $V_f \approx$ 68 knots; ≈914.4 m (≈3000 ft) pressure altitude.

Figure 9.- Comparison of model and flight recorded time history for two microphone positions. High descent velocities.

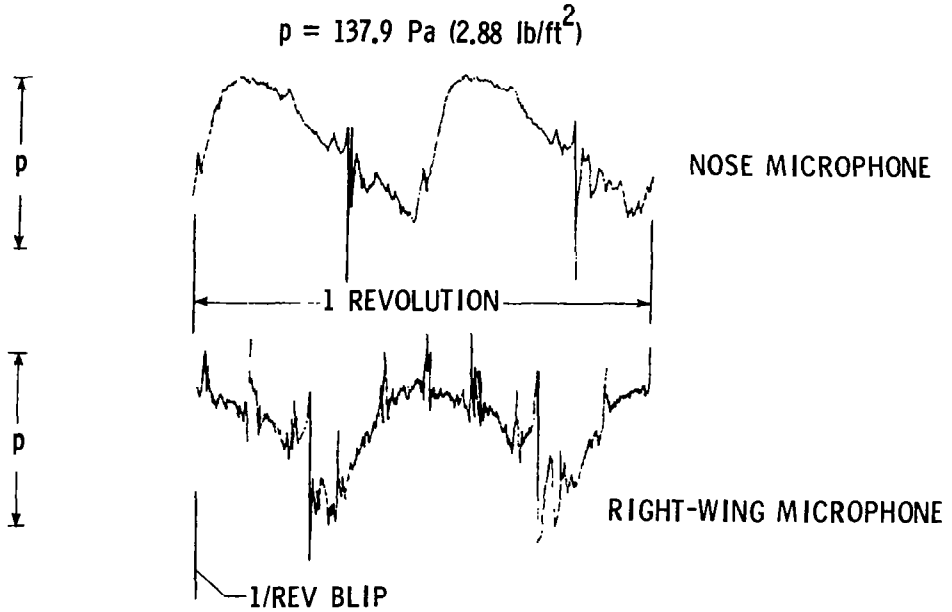

(c) Flight data; Descent velocity = 2.032 m/sec (400 ft/min); $V_f \approx 66$ knots; ≈396.2 m (≈1300 ft) pressure altitude.

Figure 9.- Concluded.